THERMOANALYTICAL INVESTIGATION OF SODIUM ACETATE TRIHYDRATE FOR APPLICATION AS A LATENT HEAT THERMAL ENERGY STORAGE MATERIAL

R. Naumann, Th. Fanghänel and *H.-H. Emons*

DEPARTMENT OF CHEMISTRY, MINING ACADEMY FREIBERG,
FREIBERG, 9200 G.D.R.

The thermal behaviour of sodium acetate trihydrate (NaAc · 3H$_2$O) was investigated by DTA, Q–TG and measurements of the solubility properties. The nucleation efficiency of Na$_4$P$_2$O$_7$ · 10H$_2$O for the crystallization of NaAc · 3H$_2$O melts is not stable over long periods. Stratification can be ascribed to the formation of anhydrous sodium acetate in the supercooled melts. Under static heat storage conditions, NaAc · 3H$_2$O and Na$_4$P$_2$O$_7$ · 10H$_2$O do not exhibit stable behaviour.

Owing to its high melting enthalpy of 264 kJ kg^{-1} [1] at the melting temperature of 58°, sodium acetate trihydrate (NaAc · 3H$_2$O) is one of a group of compounds which have frequently been proposed as latent (melting) heat storage materials [2]. However, the tendency of its melt to supercool has an adverse effect on its application. Therefore, the starting of crystallization is proposed with residual crystals [3] or foreign nucleating agents. Na$_4$P$_2$O$_7$ · 10H$_2$O [4] plays a dominant role among the foreign substances applied.

The aim of the present work is to compare the behaviours of NaAc · 3H$_2$O and Na$_4$P$_2$O$_7$ · 10H$_2$O by means of thermoanalytical methods and to discuss the conclusions with regard to possible application. The results also show the reason for the stratification in static latent heat storage units.

Experimental

The investigations were carried out on reagent grade twice-recrystallized sodium acetate trihydrate. The DTA measurements were performed with the DTA equipment manufactured by Setaram, France. Measuring equipment: cryostat, crucible holder suspensions with platinel thermocouples and closed Ti–Pd crucibles.
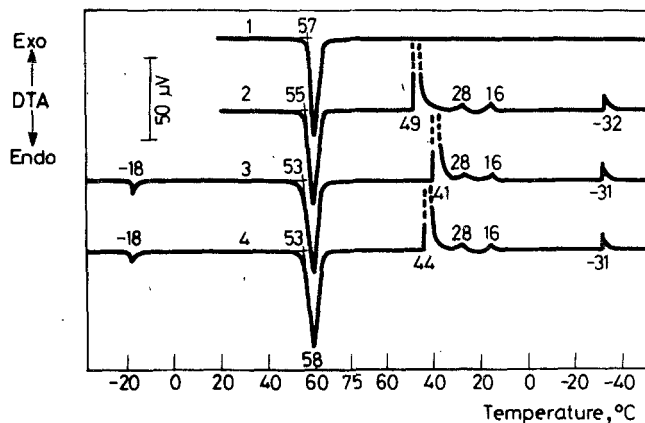
Fig. 1 DTA curves of NaAc · $3H_2O$ with and without addition of $Na_4P_2O_7$ · $10H_2O$ ($q = \pm 2$ deg min^{-1})
1 — 8.3 mg NaAc · $3H_2O$
2 — 4–9.0 mg NaAc · $3H_2O$ + 2.0 mg $Na_4P_2O_7$ · $10H_2O$
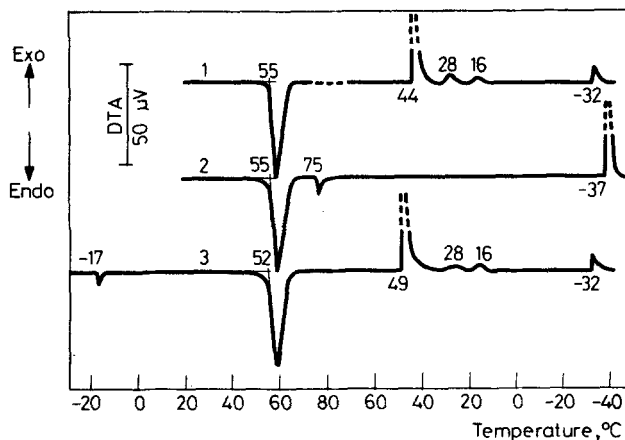
Fig. 2 DTA curves of NaAc · $3H_2O$ (10.8 mg) with $Na_4P_2O_7$ · $10H_2O$ (1.1 mg) at different limiting
temperatures ϑ_G of heating ($q = \pm 2$ deg min^{-1})·
1; 3 $\vartheta_G = 70$ °C
2    $\vartheta_G = 80$ °C

Figures 1–3 show the DTA diagrams concerning the influence of $Na_4P_2O_7$ · $10H_2O$ on the melting and solidification behaviour of NaAc · $3H_2O$ with and without superheating of the samples, and also the behaviour of pure $Na_4P_2O_7$ · $10H_2O$.

In order to investigate the solid phases formed in supercooled NaAc · $3H_2O$ melts.

solubility measurements were performed according to a method described previously [5]. Figure 4 shows the results, plotted in the well-known solubility curve for the system NaAc–H_2O.

Under quasi-isothermal and quasi-isobaric conditions, the thermal decomposition of NaAc $\cdot$ $3H_2O$ was carried out in the labyrinth crucible, using the MOM Q derivatograph. The results are shown in Fig. 5.
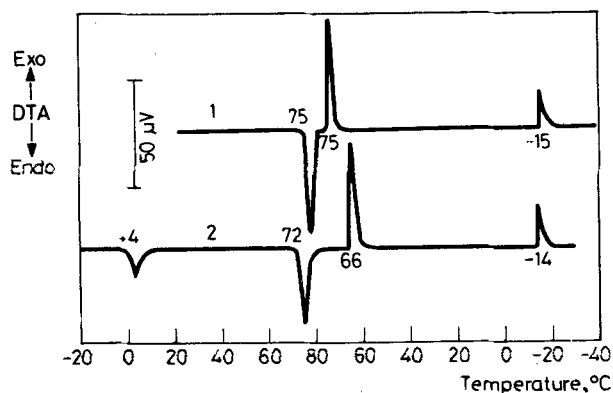

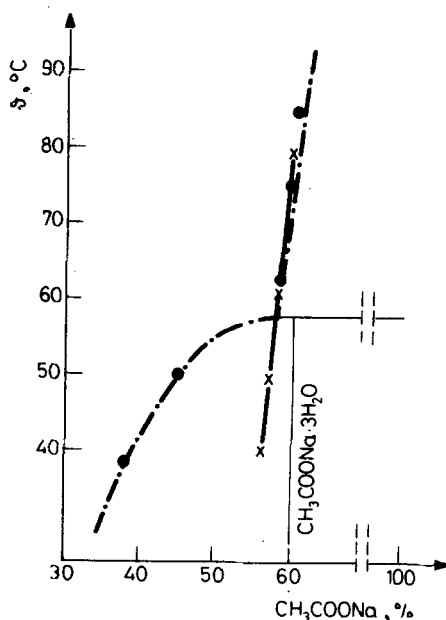Fig. 3 DTA curves of $Na_4P_2O_7 \cdot 10H_2O$ ($q = \pm 2$ deg min^{-1}, 9.6 mg)

Fig. 4 Phase diagram of the system NaAc–H_2O
—$\cdot\cdot$— (10); $\cdot$— (12); x — present work
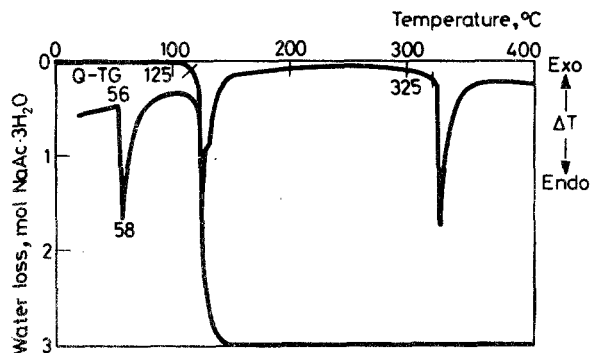
Fig. 5 Q–TG and ΔT curve of NaAc·3H$_2$O under quasi-isothermal and quasi-isobaric conditions (labyrinth crucible, Q–DTG = 0.6 mg min^{-1} TG = 100 mg, ΔT = 100 µV, program = II, sample weight = 187.1 mg)

Discussion

The DTA curves in Fig. 1 illustrate the efficiency of the nucleating agent Na$_4$P$_2$O$_7$·10H$_2$O as compared with the pure NaAc·3H$_2$O melts. In the first cycle after melting of the pure salt hydrate (ϑ_{ON} = 57°, ϑ_{peak} = 58°), no crystallization takes place in the investigated range down to −40°, while under the DTA conditions crystallization in the presence of the nucleating agent begins at 41–49°. Thus, supercooling attains a value of at most 17 deg. On increase of the sample weight to 10 g NaAc·3H$_2$O with 0.5% of nucleating agent, supercooling is reduced to 4.7 ± 0.3 deg on average, a result in agreement with that of Wada [4], who found a supercooling of 5.3 deg.

The efficiency of Na$_4$P$_2$O$_7$·10H$_2$O remains on the superheating of NaAc·3H$_2$O up to 70° (curve 1 in Fig. 2). The nucleating agent melts at higher temperatures (curve 2 in Fig. 2, ϑ_{ON} = 75°). The melts superheated beyond this temperature show high supercooling (ϑ_{ON} = −37°). Should it be possible to restart the solidification, very small amounts of Na$_4$P$_2$O$_7$·10N$_2$O would be sufficient to start crystallization with lower supercooling (curve 3 in Fig. 2). The DTA curves of Na$_4$P$_2$O$_7$·10H$_2$O confirm the behaviour of this salt hydrate in the NaAc·3H$_2$O melt (Fig. 3). In the first cycle, Na$_4$P$_2$O$_7$·10H$_2$O melts at 75° and solidifies without supercooling. Further heating and cooling cycles lead to the precipitation of Na$_4$P$_2$O$_7$ in the melt equilibrium and hence to the formation of a melt having a higher water content and a lower melting point. The additional DTA peaks at ϑ_{ON} = −14°, −15° and +4° can be attributed to the crystallization and melting processes after the eutectic line is reached at −0.4° [6].

Consequently, the absence of the nucleating efficiency of Na$_4$P$_2$O$_7$·10H$_2$O in

superheated $NaAc \cdot 3H_2O$ melts can be explained by melting of the nucleating agent. The formation of an adsorption complex with changed thermodynamic properties, as mentioned by Wada [7], seems less probable. The nucleation efficiency is also lost on longer contact with the melt, even below 75°. After 250 h at 65° during cooling, no crystallization of $NaAc \cdot 3H_2O$ is observed in the presence of 1 wt.% of $Na_4P_2O_7 \cdot 10H_2O$. Under equilibrium conditions, the transition point of $Na_4P_2O_7 \cdot 10H_2O$ to $Na_4P_2O_7$ in the ternary system $Na_4P_2O_7$–$NaAc$–H_2O is of the order of 47° [7], so that the nucleating agent $Na_4P_2O_7 \cdot 10H_2O$ cannot show any resistance to dehydration on steady contact with the melt in a static latent heat storage unit. In contrast, a nucleation efficiency exists in dynamic "Galisol" storage units, because there is no steady contact between nucleating agent an melt in this case [9].

Besides the melting and solidification effects of $NaAc \cdot 3H_2O$, further DTA peaks are shown in Figs 1–2, which can be explained by the stratification of this salt hydrate. The line of the coexisting phases in the phase diagram of $NaAc$–H_2O (Fig. 4) illustrates the presence of considerable amounts of anhydrous NaAc in supercooled $NaAc \cdot 3H_2O$ melts. Due to the precipitation of NaAc, the residual melt has a higher water content as compared with the applied composition of $NaAc \cdot 3H_2O$. Cooling of the system below $-18°$ (peritectic line) [10] causes the formation of ice (Figs 1–2). On cooling, this process is accompanied by supercooling ($\vartheta_{ON} = -31$–$32°$).

Thus, stratification of NaAc accounts for the loss of function of static $NaAc \cdot 3H_2O$ latent heat storage units. Drying processes can also lead to reduced storage capacities and thermal efficiencies. The results of quasi-isothermal thermogravimetry (Fig. 5) show that the decomposition pressure of 0.115 MPa [11] is reached at about 125°, and 3 mol H_2O is released with the formation of NaAc. the ΔT curve shows the melting point of $NaAc \cdot 3H_2O$ at $\vartheta_{ON} = 56°$ and that of NaAc at $\vartheta_{ON} = 325°$.

The summarize, it may be said that no long-term stability can be expected when $NaAc \cdot 3H_2O$ is applied in static latent heat storage units in the presence of the nucleating agent $Na_4P_2O_7 \cdot 10H_2O$. Furthermore, the phase separation phenomena have a disturbing effect, due to the formation of NaAc. On the other hand, stable heat storage behaviour is observed under dynamic GLS conditions [13, 14].

References

1 A. Pebler, Thermochim. Acta, 13 (1975) 109.

2 G. A. Lane, Solar heat storage: Latent heat materials, Vol. I. Background and scientific principles, CRC Press, Boca Raton Florida 1983.

3 E. van Galen, Thermal Storage of Solar Energy, ed. by C. den Ouden TNO and Martinus Nijhoff, The Hague (Boston) London, p. 147; CA 95 (1981) 16135810 W.

4 T. Wada and R. Yamamato, Bull. chem. Soc. Jap., 55 (1982) 3603.

5 W. Voigt, Th. Fanghänel and H.-H. Emons, Z. phys. Chem., Leipzig 266, 3 (1985) 522.

6 A. N. Kirginzev, L. N. Trushnikova and V. G. Lavrenteva, Rastvorimost' neorganičeskich veščestv v vode, Isdatelstvo Chimia 1972, p. 178.

7 T. Wada and Y. Matsuo, Bull. chem. Soc. Jap., 57 (1984) 557.

8 T. Wada and R. Yamamato, Bull. Chem. Soc. Jap., 57 (1984) 919.

9 H.-H. Emons, R. Naumann, W. Voigt, W. Stocklöw and W. Ahrens, Energy Res., 10 (1986) 69.

10 W. F. Green, J. Phys. Chem., 12 (1908) 655.

11 H.-H. Emons, T. Pohl, R. Naumann and H. Voigt, Thermische Analysenverfahren in Industrie und Forschung, Wissenschaftliche Beiträge der FSU Jena 1985, p. 65.

12 T. Wada, F. Yukotani and Y. Matsuo, Bull. Chem. Soc. Jap., 57 (1984) 1671.

13 R. Naumann and H.-H. Emons, Sitzungsberichte der AdW der DDR 3 N (1986) 31.

14 H.-H. Emons, Ö. Chem. Z., 1987, in press.

Zusammenfassung — Das thermische Verhalten von Natriumacetat-trihydrat (NaAc · $3H_2O$) wurde durch DTA, Q–TG und Löslichkeitsmessungen untersucht. Der Keimbildungseffekt von $Na_4P_2O_7$ · $10H_2O$ gegenüber NaAc · $3H_2O$ ist über längere Zeit nicht stabil. Die Schichtbildung kann zurückgeführt werden auf die Bildung von wasserfreiem NaAc in unterkühlten Schmelzen. Unter statischen Bedingungen der Wärmespeicherung zeigen NaAc · $3H_2O$ und $Na_4P_2O_7$ · $10H_2O$ kein stabiles Verhalten.

Резюме — Методами ДТА, Q—ТГ и измерением растворимости изучено термическое поведение тригидрата ацетата натрия. Степень образования центров кристаллизации в расплавах тригидрата ацетата натрия по сравнению с таковой для $Na_4P_2O_7$ · $10H_2O$, была неустойчивой в течении длительных периодов времени. Напластование может быть отнесено за счет образования безводного ацетата натрия в переохлажденных расплавах. В условиях статического теплового состояния оба соединения не показывают стабильного характера.